Experimental Research of Pressure-Volume Diagrams in a Scroll Compressor at High Speed

Xiaowen Li, Qiuhe Guo, Yusheng Hu, Huijun Wei, Yi Liao, Jia Yao, and Shuanglai Liu

Abstract The Experiment of pressure-volume (PV) diagrams is carried out to study the pressure distribution in a scroll compressor throughout the whole compression process, which is important to demonstrate the real status of the compressor during compressing operation. The analysis of pressure and efficiency based on the PV method of scroll compressor operating at high speed is presented. The composition of various loss, such as the pressure loss in suction and exhaust process, over-compression loss and indicated efficiency at different speeds and operation conditions are finally obtained. The results show that the suction and exhaust pressure loss increase rapidly with the rising of rotation speed, which leads to the decrease of indicated and volumetric efficiency. The composition of loss is quite different from low speed to high speed. The research is useful to understand various important phenomena and improve our design of scroll compressor at high speed.

Keywords Scroll compressor · PV diagram · High speed

1 Introduction

The development of commercial refrigeration system takes energy saving and environmental protection as the main melody. Compressor is the core component of refrigeration system, and its performance directly affects the energy-saving efficiency of the whole system. Inverter scroll compressors are widely used in domestic

X. Li (✉) · Y. Hu · H. Wei · Y. Liao
State Key Laboratory of Air-Conditioning Equipment and System Energy Conservation, Jinji West Rd, Zhuhai 519070, People's Republic of China
e-mail: lxw86119@163.com

X. Li · Y. Hu · H. Wei · J. Yao
Guangdong Key Laboratory of Refrigeration Equipment and Energy Conservation Technology, Zhuhai 519070, People's Republic of China

X. Li · Q. Guo · Y. Hu · H. Wei · S. Liu
Gree Electric Appliances, Inc. of Zhuhai, Zhuhai 519070, People's Republic of China

M. Read et al. (eds.), *13th International Conference on Compressors and Their Systems*, Springer Proceedings in Energy, https://doi.org/10.1007/978-3-031-42663-6_26

and commercial refrigeration systems with large capacity, due to their high efficiency, low torque variation, noiseless operation, low vibration and smooth operation. Finding out the internal operating characteristics of inverter scroll compressors at different frequencies is particularly important for high-efficient optimization design of compressors.

Pressure and volume change law test (PV diagram measurement) on the inside of the compressor is an important means to understand the internal working characteristics of the compressor. At present, the existing papers mainly focus on rotary compressors, and there are relatively few studies on inverter scroll compressors.

In this paper, by testing the PV characteristics of the inverter scroll compressor with high and low frequencies, the characteristics of scroll compressors are compared and the relative variation law is analyzed, which provides the basis and reference for the optimization design of scroll compressors at high speed.

2 Theory of Experiment

2.1 Thermodynamic Model of Compression Chambers

For compression chamber, mass and energy conservation equations are deduced to describe the thermodynamics state. And between chambers, an isentropic nozzle model of one-dimensional compressible flow is used to determine the mass and energy exchange from flank and radial clearance.

According to the conservation of mass and energy [1], the equations can be written as:

$$\frac{\mathrm{d}m}{\mathrm{d}\theta} = \frac{1}{\omega}\left(\dot{m}_i - \dot{m}_o\right) \tag{1}$$

$$\frac{\mathrm{d}T}{d\theta} = \frac{\frac{1}{\omega}\left(\dot{m}_i(h_i - h) - \dot{m}_o(h_o - h)\right) - \left(\left(\frac{\partial h}{\partial \upsilon}\right)_T - \left(\frac{\partial p}{\partial \upsilon}\right)_T \frac{V}{m}\right)\left(\frac{\mathrm{d}V}{\mathrm{d}\theta} - \frac{V}{m}\frac{\mathrm{d}m}{e\theta}\right)}{m\left(\frac{\partial h}{\partial T}\right)_v - V\left(\frac{\partial p}{\partial T}\right)_v} \tag{2}$$

The isentropic nozzle model is used to calculate the mass flow rate through the clearances between fixed and orbiting scroll wrap [2], which can be written as

$$\dot{m} = C_\mathrm{d}\rho_\mathrm{up}A\left(\frac{2\gamma}{\gamma-1}\frac{p_\mathrm{up}}{\rho_\mathrm{up}}\left(\left(\frac{p_\mathrm{down}}{p_\mathrm{up}}\right)^{\frac{2}{\gamma}} - \left(\frac{p_\mathrm{down}}{p_\mathrm{up}}\right)^{\frac{\gamma+1}{\gamma}}\right)\right)^{\frac{1}{2}} \text{for}\ \frac{p_\mathrm{down}}{p_\mathrm{up}} \geq \left(\frac{2}{\gamma+1}\right)^{\frac{\gamma}{\gamma-1}} \tag{3}$$

$$\dot{m} = C_\mathrm{d}\rho_\mathrm{up}A\left(\frac{\gamma p_\mathrm{up}}{\rho_\mathrm{up}}\left(\frac{2}{\gamma+1}\right)^{\frac{\gamma+1}{\gamma-1}}\right)^{\frac{1}{2}} \text{for}\frac{p_\mathrm{down}}{p_\mathrm{up}} < \left(\frac{2}{\gamma+1}\right)^{\frac{\gamma}{\gamma-1}} \tag{4}$$

2.2 Efficiency of Compression Chambers

Based on the law of thermodynamics, the enthalpy difference change during the suction process satisfies the relation of $\Delta h = \Delta q + \Delta w$. If the heat exchange between the refrigerant and the environment in the suction process is ignored, the flow loss Δw caused by the viscous friction of the refrigerant during the charging process are all converted into heat and absorbed by the refrigerant, now the equation is known as $\Delta q + \Delta w = 0$, so the enthalpy value remains unchanged during the flow process. In addition, the temperature remains constant if h ($h = C_p * T$) keeps invariant. The pressure of the refrigerant decreases while the temperature remains unchanged, thus the density of coolant decreases. Besides, the aspirated volume of the compressor is fixed, it will inevitably lead to a decrease of inspiratory mass and volumetric efficiency when the density of the refrigerant decreases.

The theoretical mass of refrigerant is denoted by ms $= \rho_s V_s$. The pressure (P) somewhere in the suction process can be obtained by PV diagram measurement, subsequently, the density (ρ) can be calculated from the pressure (P), temperature (T_s) and physical property of the refrigerant, then the actual mass can be written as $m = \rho V_s$ [2, 3]. Volume efficiency loss due to flow losses is given by

$$\eta_i = (\rho_s V_s - \rho V_s)/(\rho_s V_s) = 1 - \rho/\rho_s \tag{5}$$

Figure 1 shows the indicated work division diagram of compressor, where P_s is the theoretical suction pressure, P_d is the theoretical exhaust pressure, P_{s1} is the measured suction pressure, P_{d1} is the measured exhaust pressure, V_h is the actual effective volume of the compressor, V_d is the discharge port open volume of the compressor, n is the rotary speed, ① is the theoretical work of adiabatic compression, ② is suction pressure loss. ③ represents other losses in the compression process (mainly including under-compression loss, leakage loss, heat loss, etc.), and ④ is the exhaust pressure loss (including loss of over compress, loss of pump body's discharge port, the loss of exhaust flow).The pressure loss during the suction and discharge process of the compressor is as follows

$$\Delta P_{\mathrm{i}} = \overline{n}/60 \int_0^{V_h} [P_S - P_s(\theta)]\mathrm{d}V \tag{6}$$

$$\Delta P_0 = \overline{n}/60 \int_0^{V_d} [P_d(\theta) - P_d]\mathrm{d}V \tag{7}$$

According to the pressure calculation formula, P is defined as

$$P = P_{\mathrm{s}}(V_{\mathrm{s}}/V)^{\mathrm{n}} \tag{8}$$

Taking the closure pressure (P_0) of suction process and compression index n as unknowns, the P–V data of the compression stage of the test can be used to fit the

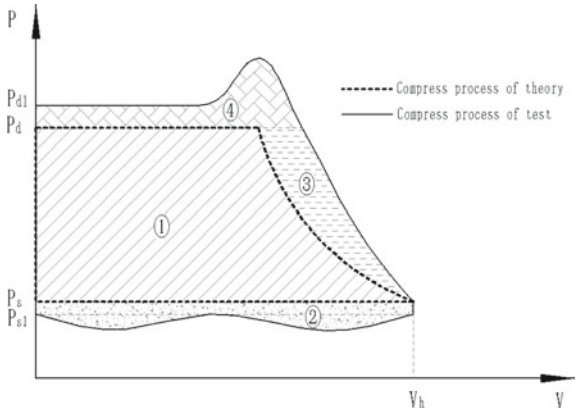

Fig. 1 P-V schematic diagram of scroll compressor

closure pressure (P_0) of suction process and compression index (n) at each operation condition. By substituting the fitted parameters into the pressure calculation formula, the actual pressure change of the compression chambers in the compression stage can be calculated more accurately.

3 Test Method and Equipment

3.1 Testing Compressor

Multiple displacement and pressure sensors need to be installed to monitor pressure and volume changes in PV diagram measurement. The compressor needs to be specially made, which is a detachable compressor with upper and lower covers, as shown in Fig. 2. The data of pressure (P) and displacement (V) are respectively collected by the acquisition card (NI: 9239), and the PV curve diagram of the operation process is obtained by post-processing method.

3.2 Pressure Measurement

Pressure sensors (Kulite: XTL-142B-190 M-50barA, USA) are inserted into the fixed scroll of the pump body. Four pressure sensors are arranged in the inner and outer compression chambers of the pump body respectively, and every four sensors monitor a complete compression cycle, as shown in Fig. 3. The connecting wire is connected from the flange plate on the upper cover of the compressor and the experiment is tested in multiple groups.

Fig. 2 Picture of testing compressor

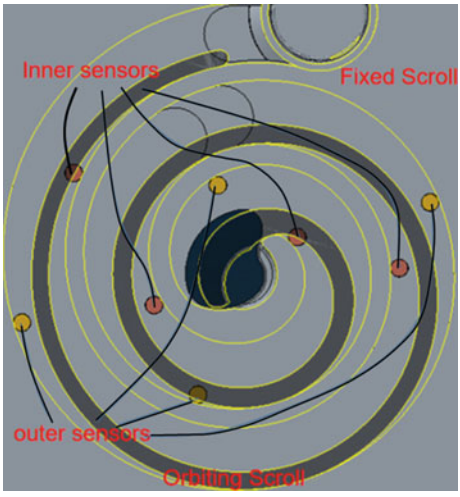

Fig. 3 Location of pressure sensors

3.3 Volume Measurement

By sensing the rotation angle of the gear flange mounted on the compressor with a displacement sensor (Del: DT3010-M, Germany), and then the volume can be obtained by the relevant calculation. The newly designed displacement induction gear flange is assembled on the shafting system, meanwhile, the pressure sensor goes deep into the shell and the wire is connected from the shell flange, as shown in Fig. 4.

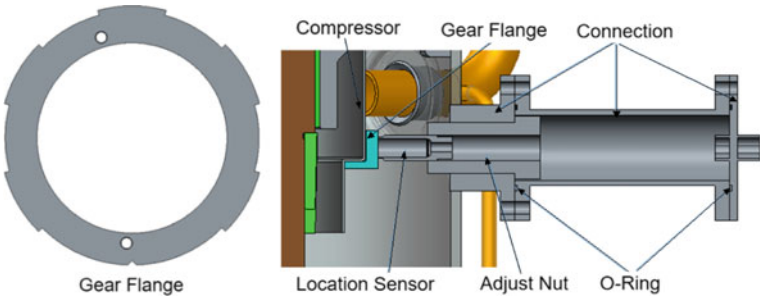

Fig. 4 Illustration of location sensor

Table 1 Operation condition for experiments

Load condition	Suction pressure (MPa)	Discharge pressure (MPa)	Suction temperature (°C)	Frequency (Hz)	Refrigerant
1	0.634	2.086	− 2	123/199	R410A
2	0.850	1.788	7	65/106	
3	0.877	1.652	8	28/46	

4 Results and Discussion

4.1 Experiment Condition

According to the enterprise standard, the conditions in Table 1 are selected for test comparison, and the pressure ratio is from large to small. The ultrahigh electric motor frequency(Full text abbreviation: frequency) of 199 Hz is taken as the upper limit, and the PV curves of high and low frequencies under various working conditions are compared respectively to analyze the loss ratio changes of each module with high and low frequencies(unit volume:98 cc). All experiments are implemented in a compressor calorimeter.

4.2 Data Analysis

The test results are shown in Figs. 5, 6 and 7 (All the measurement results of an inner compression chamber). Under the high-frequency working condition 1 (Fig. 5), and the actual exhaust pressure at the theoretical discharge angle is lower than the theoretical exhaust pressure. Meanwhile, the pressure rises sharply after the opening of the discharge port, there is an under-compression phenomenon of high-pressure gas return, and the under-compression phenomenon is aggravated under ultra-high frequency condition. On the other hand, the actual suction pressure is lower than

the theoretical suction pressure and with suction loss. Under the condition of ultra-high frequency, suction loss increases. The actual exhaust pressure at the theoretical discharge angle of working condition 2 and 3 is higher than the theoretical exhaust pressure. When the pressure reaches the exhaust pressure, the orbiting scroll does not reach the exhaust angle, and there is the over-compression phenomenon. With the increase of frequency, the over-compression phenomenon becomes worse [4].

The actual suction pressure in low frequency is higher than the theoretical suction pressure, and the "precompression" characteristic phenomenon of scroll is obvious, and the "precompression" phenomenon decreases with the increase of frequency. (Precompression: When the suction chamber of scroll compressor is close to closure, the volume of chamber gradually decreases, and the gap at the closure point of the profile line also gradually decreases. When the gap decreases to a certain extent, the influence of leakage through the gap is small, and the suction chamber can be considered as a closed chamber. With the rotation of the orbiting scroll, the volume

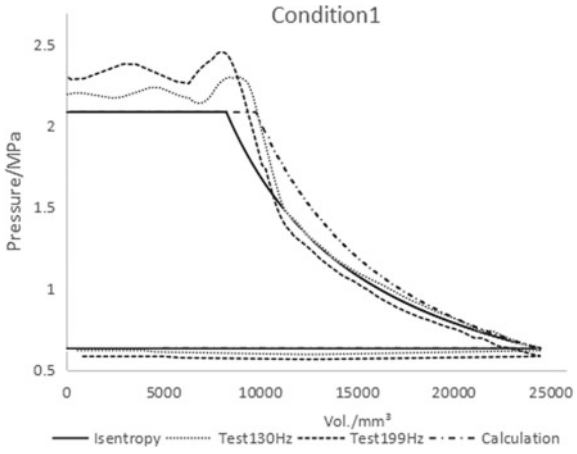

Fig. 5 PV diagram of condition 1

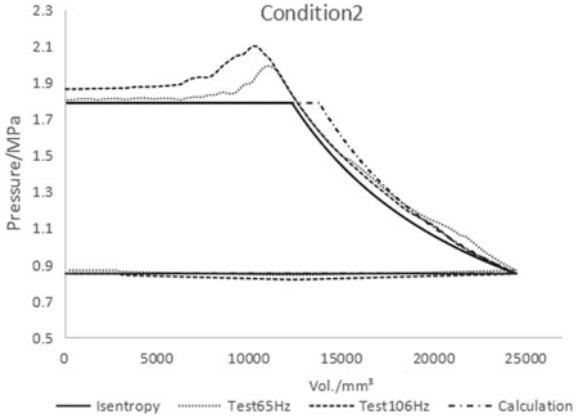

Fig. 6 PV diagram of condition 2

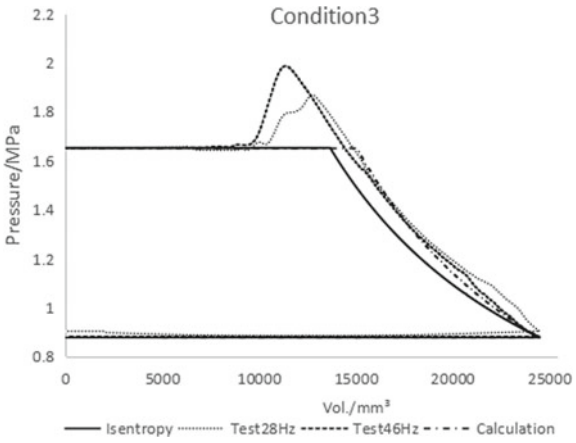

Fig. 7 PV diagram of condition 3

of the chamber gradually decreases and the pressure gradually rises, that is, the compression has begun before the inspiratory closure.

By calculating the area of each loss module in Figs. 5, 6 and 7 and summarizing statistics, the comparison Figure of loss ratio is obtained, as shown in Figs. 8, 9 and 10. The ratio of over (under)-compression and the discharge loss of pump body keepsz direct ratio with frequency, the loss of exhaust flow keep direct ratio with frequency and only occurs in mid-low frequencies. The other losses (leakage and heat loss, etc.) are keep inverse ratio with frequency. Under the ultra-high-frequency condition 1, the over (under)-compression and discharge loss account for the main part of the total loss. The indicated efficiency (The ratio of theoretical work of adiabatic cycle to actual cycle) does not change significantly in low frequency, decreases in high frequency, and decrease range enhances in ultra-high frequency, as shown in Fig. 11.

5 Conclusions

(1) The over-compression and under-compression of scroll compressor are difficult to avoid under various working conditions. With the increase of frequency, the actual discharge angle increases.
(2) Different frequencies have a great impact on suction-exhaust process. The deviation of suction and exhaust conditions increases in ultra-high frequency conditions, so the suction and exhaust structures need to be redesigned and optimized.

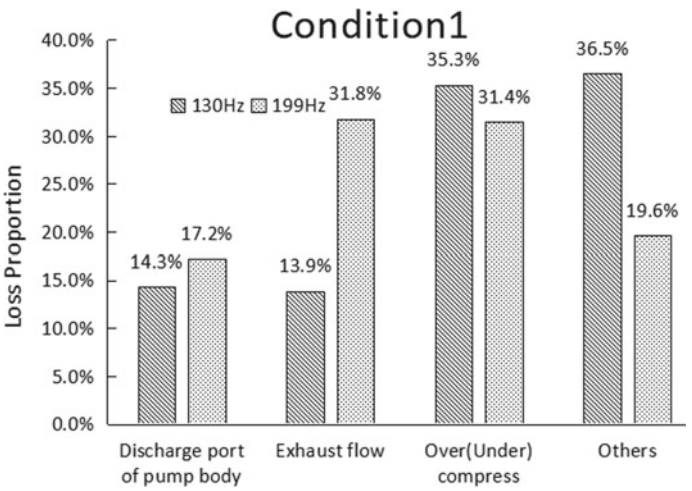

Fig. 8 Loss ratio of condition 1

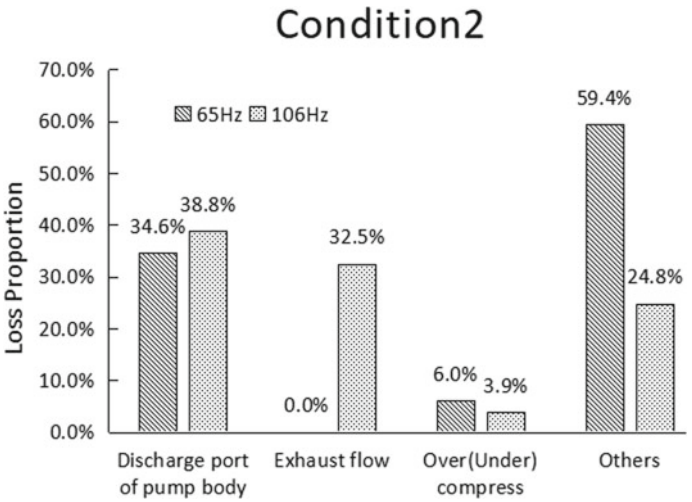

Fig. 9 Loss ratio of condition 2

(3) The proportion of exhaust loss and over (under)-compression loss are keep direct ratio with the frequency, and the proportion of ultra-high frequency accounts for the main part of the total loss. There is no significant change in indicated efficiency at low frequencies, while indicated efficiency decreases at high frequency and it decreases intensified at ultra-high frequency.

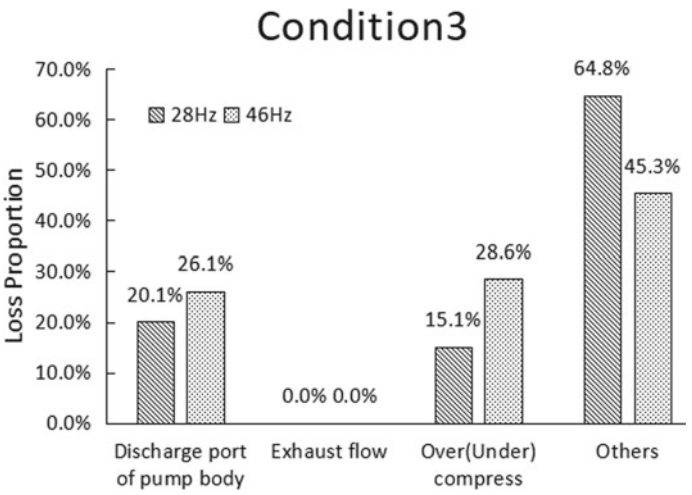

Fig. 10 Loss ratio of condition 3

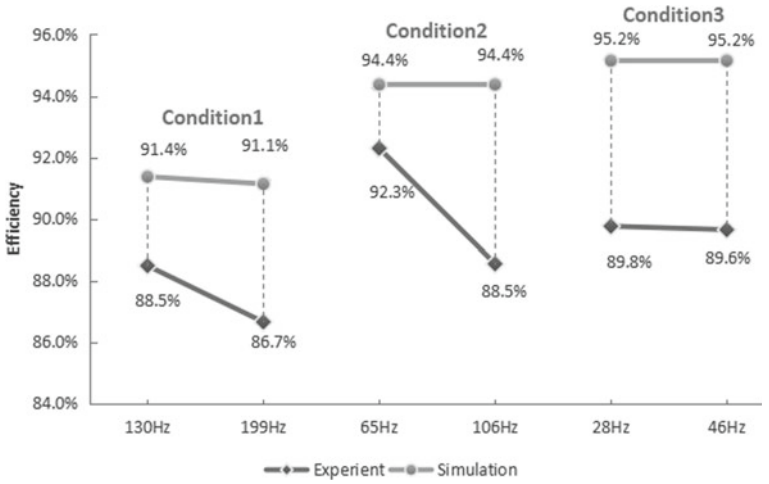

Fig. 11 Indicated efficiency comparison

Nomenclature

p	Pressure (Pa)
T	Temperature (K)
V	Volume (m^3)
m	Mass (kg)
ρ	Density (kg $\times$ m^{-3})
A	Area (m^2)

n	Compress exponential (–)
η	Efficiency (%)
C_P	Mobar heat capacity at constant pressure (J/(mol × K))
m	Mass flow rate (kg × s^{-1})
h	Specific enthalpy (J × kg^{-1})
u	Specific volume (m^3 × kg^{-1})
θ	Orbiting angle (rad)
ω	Angular speed (rad × s^{-1}
γ	Polytropic index (–)
v	Velocity (m × s^{-1})
C	Efficiency (%)

Subscripts

i	In
O	Out
n	Natural frequency
S	Suction gas
Up	Upstream
$down$	Downstream
s	Suction gas
h	Heat

References

1. X. Jia, L. Shuanglai, L. Yun, S. Caixia, The experimental and numerical study of discharge valves in scroll compressor. J. Chem. Eng. **50**(12), 43–44 (2022)
2. Y.C. Park, Y. Kim, H. Cho, Thermodynamic analysis on the performance of a variable speed scroll compressor with refrigerant injection. Int. J. of Refrigeration **25**(8), 1072–1082 (2002)
3. Wu. Jianhua, Y. Li, G. Wang et al., Measurement of Indicated Diagram and Performance Analysis of Propane Rolling Piston Compressor. J. Xi'an Jiaotong Uni. **3**, 6–11 (2014)
4. K.C. Moun,Y. Tae-Hwan, K. Tae-Jong et al., Performance evaluation of rotary compressor with special attention to the accuracy of P-V diagram, in *Proceedings of the International Compressor Engineering Conference.* (Purdue University, USA 1990), pp. 442–449